

X-ray Polarimetry: a new window on the high energy sky

R. Bellazzini^a, F. Muleri^{b,*}

^a*INFN sez. Pisa, Largo B. Pontecorvo 3, I-56127 Pisa, Italy*

^b*IASF/INAF, Via del Fosso del Cavaliere 100, I-00133 Roma, Italy*

Abstract

Polarimetry is widely considered a powerful observational technique in X-ray astronomy, useful to enhance our understanding of the emission mechanisms, geometry and magnetic field arrangement of many compact objects. However, the lack of suitable sensitive instrumentation in the X-ray energy band has been the limiting factor for its development in the last three decades. Up to now, polarization measurements have been made exclusively with Bragg diffraction at 45° or Compton scattering at 90° and the only unambiguous detection of X-ray polarization has been obtained for one of the brightest object in the X-ray sky, the Crab Nebula. Only recently, with the development of a new class of high sensitivity imaging detectors, the possibility to exploit the photoemission process to measure the photon polarization has become a reality. We will report on the performance of an imaging X-ray polarimeter based on photoelectric effect. The device derives the polarization information from the track of the photoelectrons imaged by a finely subdivided Gas Pixel Detector. It has a great sensitivity even with telescopes of modest area and can perform simultaneously good imaging, moderate spectroscopy and high rate timing. Being truly 2D it is non-dispersive and does not require any rotation. This device is included in the scientific payload of many proposals of satellite mission which have the potential to unveil polarimetry also in X-rays in a few years.

Keywords: X-rays, Gas Detectors, Polarimetry

PACS: 29.40.Cs, 07.85.Fv, 95.55.Ka, 95.75.Hi

1. Introduction

X-ray polarimetry was born together with X-ray astronomy. First pioneering experiments were carried out in the seventies with polarimeters based on Bragg diffraction at 45° or Compton scattering at 90° on-board sounding rockets and first results were quite encouraging: already Novick et al. (Novick et al., 1972)

*Corresponding author.

Email address: fabio.muleri@iasf-roma.inaf.it (F. Muleri)

reported a marginal yet significant detection of polarization in the emission of the Crab Nebula, confirmed a few years later with high significance by the Bragg polarimeter on-board OSO-8 (Weisskopf et al., 1978). This observation was favoured by the intense flux of the source and the high degree of polarization, signature of synchrotron emission ($\mathcal{P} \approx 20\%$), and, as a matter of fact, it has remained unique. Only upper limits were derived for other astrophysical objects because of the combined effect of a lower flux and an inferior polarization degree (Long et al., 1979; Hughes et al., 1984).

Unfortunately no other tool dedicated to X-ray polarimetry has been launched after OSO-8. The Stellar X-ray Polarimeter on-board the Spectrum-X-Gamma mission, although the flight model was ready and calibrated, was never put in orbit because of the collapse of Soviet System. The proposals to include polarimeters on-board observatories like XMM or AXAF, which were the only opportunities to have a sufficient collecting area, has never been carried out: instruments exploiting Bragg diffraction or Compton scattering didn't look attractive because, while imaging and spectroscopic devices promised an enormous increase of sensitivity, polarimetry would be limited to a few bright sources even in the focus of these large telescopes. Moreover "classical" polarimeters were cumbersome because they need to be rotated around the direction of incident photons.

Conversely, the lack of experimental feedback has not prevented the development of a rich literature on the basis of which we expect that almost all sources in the X-ray sky should emit partially polarized radiation (for reviews see Rees, 1975; Meszaros et al., 1988; Weisskopf et al., 2009). The study of the state of polarization would unveil the magnetic field and the geometry of the sources and it would pinpoint the emission processes at work, discriminating among competitive models otherwise equivalent from the spectral or the timing point of view. This is the case of emission geometry in pulsars (Dyks et al., 2004) or X-ray pulsars in binaries (Meszaros et al., 1988), but peculiar signatures are also expected for isolated neutron stars because of the different opacity of the two normal modes in a magnetized plasma and because of vacuum polarization (Canuto et al., 1971; Pavlov and Zavlin, 2000; Lai and Ho, 2002; Heyl et al., 2003). Moreover polarimetry is a powerful probe to investigate fundamental theories. General Relativity in the strong field regime can be tested by means of the rotation of the plane of polarization with energy expected for stellar-mass black-holes, and the amplitude of the effect would provide a measurement of the spin (Stark and Connors, 1977; Dovčiak et al., 2008; Li et al., 2009). Instead a rotation of the polarization angle increasing with distance could tightly constrain the vacuum birefringence expected in some theories of Quantum Gravity (Gambini and Pullin, 1999; Mitrofanov, 2003; Kaaret, 2004).

As a proof for the impelling interest in X-ray polarimetry, many authors have attempted to extract the polarization information as a byproduct of existing imaging devices. By selecting those events which are scattered and detected between two adjacent pixels, any imaging instrument is in principle a Compton polarimeter because the line connecting the hit pixels approximates the scattering direction. While some results have been achieved for the Crab Nebula

with INTEGRAL (Dean et al., 2008; Forot et al., 2008), measurements of this kind may be affected by strong systematic effects, are limited to strong sources because of the low Compton scattering probability in the detector and, in many case, remains questionable (Coburn and Boggs, 2003; Rutledge and Fox, 2004).

Today gas detectors able to image the tracks of photoelectrons provide a valuable alternative to classical techniques. Basically, they promise a jump in sensitivity thanks to the much higher capability to collect photons, obtained with a larger energy band with respect to Bragg polarimeters and a lower energy threshold than Compton instruments. In the following we present the Gas Pixel Detector (GPD hereafter), one of the first devices able to resolve photoelectron paths in a gas mixture at atmospheric pressure even at low energy and specifically designed for astrophysical application.

2. Photoelectric effect

Photoelectric effect is a good analyzer of polarization and a perfect one in case of absorption of spherically symmetric electron orbitals. The differential cross section of the interaction for the K-shell is (Heitler, 1954):

$$\frac{d\sigma_{ph}^K}{d\Omega} = r_0^2 \alpha^4 Z^5 \left(\frac{m_e c^2}{E} \right)^{\frac{7}{2}} \frac{4\sqrt{2} \sin^2 \theta \cos^2 \phi}{(1 - \beta \cos \theta)^4} \propto \frac{\sin^2 \theta \cos^2 \phi}{(1 - \beta \cos \theta)^4}, \quad (1)$$

where β is the photoelectron velocity in units of c and r_0 is the classical electron radius. The angles θ and ϕ are those that the initial direction of the photoelectron makes with the direction of the absorbed photon and its electric field, respectively. The probability of photoelectron emission in a certain azimuthal direction ϕ is modulated as a \cos^2 function and hence polarized photons cause a modulation in the direction of ejection, the peak corresponding to the direction of polarization.

If other electronic shells are considered, the lack of spherical symmetry requires to include in Equation (1) an asymmetry factor b (Ghosh, 1983):

$$\frac{d\sigma_{ph}}{d\Omega} = \frac{\sigma_{ph}^{tot}}{4\pi} \left[1 + \frac{b}{2} \left(\frac{3 \sin^2 \theta \cos^2 \phi}{(1 + \beta \cos \theta)^4} - 1 \right) \right]. \quad (2)$$

The value of b is a function of energy (Yeh, 1993) but in general $b \leq 2$, where the equality holds for spherical shells and hence Equation 2 collapses to Equation 1.

In the following we will assume that the \cos^2 modulation is complete for completely polarized photons since photoelectric polarimeters in general work above the K-shell energy threshold and this makes negligible the contribution of not spherical shells. For example, in the working band of the GPD 99% of photons are absorbed by 1s or 2s orbitals, which are completely modulated.

3. The Gas Pixel Detector

The Gas Pixel Detector has been developed and is continuously improved by INFN-Pisa in collaboration with INAF/IASF-Rome (Costa et al., 2001; Bellazzini et al.,

2006, 2007). It is composed of a sealed gas cell, 1 or 2 cm thick, enclosed by a 50 μm beryllium window, a GEM (Gas Electron Multiplier, Sauli, 1997) and a finely subdivided pixelized detector (see Figure 1a). When an X-ray photon is absorbed in the gas cell, a photoelectron is ejected, propagates in the gas losing energy by ionization and is eventually stopped after a path of a few hundreds of microns (track). Alongside the photoelectron it is likely the emission of an Auger electron: the latter must be distinguished since its direction of ejection is isotropic and doesn't bring memory of polarization. This implies that a hard limit to the energy threshold is about twice the binding K-shell energy of the absorbing gas component because in this case the track of photoelectron is more energetic and hence longer. The electrons produced along the path of the photoelectron (and of the Auger electron) drift in the gas and are amplified thanks to the electric field generated by the GEM. Eventually the charge distribution is collected on the pixelated top metal layer of a $15 \times 15 \text{ mm}^2$ VLSI ASIC which provides a true 2D image of the photoelectron track. This latter component, realized in 0.18 μm CMOS technology, is the actual breakthrough of the instrument: the 105,600 pixels are arranged in hexagonal pattern at 50 μm pitch and are connected to full and independent electronics chains, which are built immediately below the top layer of the ASIC and includes pre-amplifier, shaping amplifier, sample and hold and multiplexer. An important characteristic of the ASIC is that it has self-triggering capabilities which allow to read-out only a small region enclosing those pixels which were actually hit. The whole 300×352 matrix is divided into 16 (or 8) clusters, each further subdivided into mini-clusters of 4 pixels. When the charge collected by a mini-cluster is higher than a threshold of ~ 2000 electrons, corresponding to a few electrons before GEM amplification, a trigger is generated and the rectangular region of 10 or 20 pixels (externally selectable) around the mini-cluster(s) which triggered, called Region Of Interest (ROI), is fetched and read-out. Immediately after the event (delay of a few μs), the pedestals in the ROI are read-out (one or more times) and subtracted to data. The electronic noise of the pixels is only 50 electrons ENC (Bellazzini et al., 2006).

The first part of the track produces a lower charge density than the final one, since energy losses by ionization are inversely proportional to the energy E , but the former contains the large part of the information on polarization. Elastic scatterings, occurring with a probability $\propto Z^2/E^2$ (Z is the average atomic number of the mixture), isotropize the direction of photoelectrons which eventually loses any correlation with the polarization. Hence is of fundamental importance to combine a good quantum efficiency and the capability to resolve and distinguish the initial part of the track. The small pixel size of the ASIC and the low diffusion of the mixtures we used, composed of helium, neon or argon and dimethyl ether (DME hereafter), assure that even at a few keV the photoelectron tracks are well resolved. Moreover we have developed an algorithm which can effectively reconstruct the initial direction of emission and the impact point by analyzing only the initial part of the photoelectron path (Bellazzini et al., 2003). This is distinguished by those hit pixels which are at the edge of the track with the lower ionization density: by a proper selection and weight of the

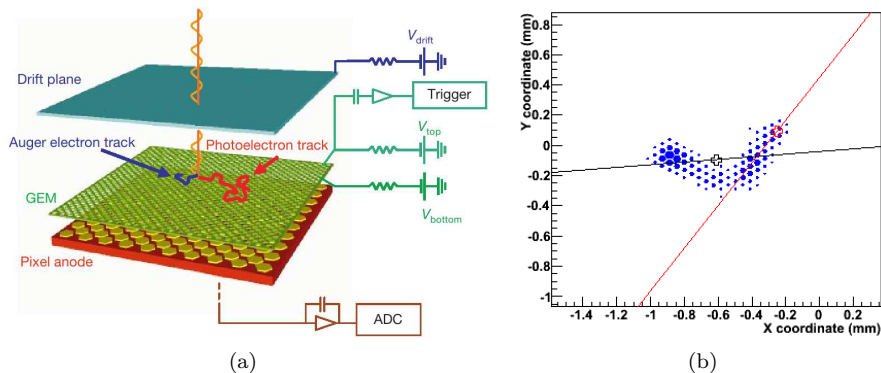


Figure 1: (a) Principle of operation of the Gas Pixel Detector (Costa et al., 2001). (b) An example of a real track at 5.2 keV. The reconstructed direction of emission and the impact point are the red line and the red cross respectively.

contribution of each pixel, the best estimate of the direction of emission and of the absorption point are derived as the direction which maximizes the second moment and the center of mass of the charge distribution, respectively.

An image of a real track at 5.2 keV in pure DME at 0.8 bar is reported in Figure 1b. The effect of a large scattering is clearly resolved as the denser region where photoelectron is eventually stopped (Bragg peak). The discrimination of the first part of the track allows for a reconstruction of the direction of emission and of the absorption point (depicted as the line and the cross in red) by far better than if the entire track is analyzed (in black in Figure). The possibility to measure the impact point, with a resolution of the order of $150 \mu\text{m}$, gives to the GPD the unique possibility among gas polarimeters to image the source and reduce the background in the focus of a telescope to a negligible level. Moreover, as any conventional gas counter, the energy and the time of the event are also available. Goal spectroscopic and timing resolutions are 20% at 5.9 keV and $\sim 8 \mu\text{s}$, achieved by reading-out the signal of the GEM together with that of the ASIC. However even current spectral performance, obtained by summing the charge collected in hit pixels, is already encouraging, 24% at 5.9 keV (Muleri et al., 2009).

The GPD is assembled with low-outgassing materials in collaboration with Oxford Instruments Analytical Oy and it doesn't show any significant degradation after more than 1 year of continuous operation. The gas cell is sealed and this allows to build a very compact instrument: the detector and the back-end electronics currently in use in our laboratory are in a box $140 \times 190 \times 70 \text{ mm}^3$ which weights 1.6 kg and the power consumption is $\leq 5 \text{ W}$ (see Figure 2). Notwithstanding the mixture can be refilled to test different configurations in view of the great importance of this choice. Currently, best performance in the energy range 2-10 keV, where first use is expected, is achieved with a mixture of helium and DME at 1 atm, but we are also studying mixtures of argon to

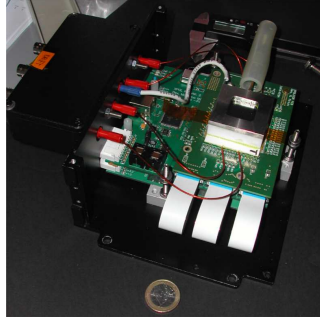


Figure 2: A picture of the GPD detector and of the back-end electronics.

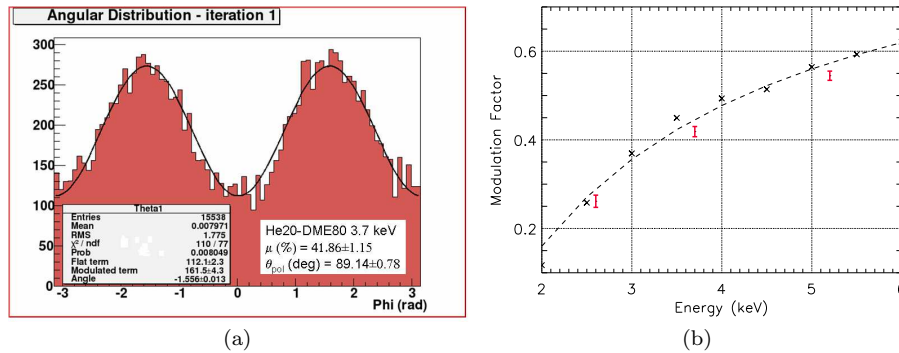


Figure 3: (a) Modulation curve for a mixture of helium and DME and completely polarized photons at 3.7 keV. (b) Modulation factor measured at 2.6, 3.7 and 5.2 keV (red points) compared to the values expected from Monte Carlo simulations (crosses). The dashed line is a fit to Monte Carlo data (both Figures after Muleri et al., 2008).

extend the energy range up to ~ 35 keV (see Section 4).

An example of the histogram of emission directions as a function of the azimuthal angle (modulation curve) is shown in Figure 3a for 3.7 keV polarized photons. The amplitude of the modulation measured at 2.6, 3.7 and 5.2 keV for completely polarized photons (modulation factor) is consistent with the values expected on the basis of Monte Carlo simulations (see Figure 3b).

4. Satellite missions

There aren't critical issues for the use of GPD on-board space satellites and the instrument has a very high readiness level. The VLSI technology naturally withstands high levels of radiation and tests at the Heavy Ion Medical Accelerator in Chiba (HIMAC) confirmed that performance remains nominal after

the irradiation of iron ions corresponding to several years in orbit. There is a long heritage in avoiding and eventually controlling pollution of sealed gases on-board space satellites. The detector survived vibrations and thermo-vacuum tests between -15 and 45°C and both the GEM and the $50\ \mu\text{m}$ thin beryllium window are compatible with the use in space. The gas amplification gain is maintained low thanks to the low pixels noise and this reduces the probability of destructive discharges.

The imaging capability of the GPD will be exploited at best with the use of an X-ray optics. This will assure (i) an adequate collecting area, (ii) the possibility to resolve extended sources and (iii) to reduce to a negligible level the background, expected to be more than two orders of magnitude lower than the fainter source accessible to X-ray polarimetry. The intrinsic azimuthal symmetry of the instrument makes the systematic effects much lower than 1%, Bellazzini et al. (Bellazzini and Spandre, 2010) reported that for ^{55}Fe 5.9 keV unpolarized photons the residual modulation is $0.18\pm 0.14\%$. This allows to avoid the rotation of the instrument which is an odd complication to the design of modern three-axis stabilized satellites.

The GPD is currently included in several proposals of mission which have passed a certain level of selection (see Table 1). One possibility is *XPOL* on-board the large satellite *International X-ray Observatory* (IXO), which allows to exploit a huge collecting area ($1.5\ \text{m}^2$ at 3 keV) and achieve a fine angular resolution, 5 arcsec including the blurring due to inclined penetration of photons in the gas cell. Even if only a small fraction of the observation time would be dedicated to *XPOL*, a minimum detectable polarization (MDP) of 1% at the 99% confidence level could be reached within 100 ks for 1 mCrab source, thus making possible polarimetry even of faint extragalactic sources (Costa et al., 2008; Bellazzini et al., 2010 in press). Nevertheless the sensitivity of the GPD would allow to achieve a wealth of results even with a less demanding mission profile. Using a telescope of modest area dedicated to polarimetry, tens of galactic and extragalactic bright sources would be accessible to the level of 1% in a few days of observation. Such a small missions could be placed in orbit with a moderate cost and well before IXO, whose launch is expected in 2021, with the additional advantage to drive the development and the observations of the latter mission.

To the pathfinder mission profile belong missions like *POLARIX* (Costa et al., 2006, 2009), an Italian mission dedicated to X-ray polarimetry between 2 and 10 keV which concluded a phase A study at the end of 2008 and it's currently waiting for the possible selection to launch by the Italian Space Agency (ASI), and the polarimeters on-board the Chinese mission *HXMT* (Soffitta et al., 2008). These missions (see Table 1) exploit a small cluster of identical telescopes to reduce costs. While summing data from more detectors doesn't impact on sensitivity thanks to the negligible background, the replica of identical optics allows to achieve an equivalent area with a smaller number of shells, whose production compose the large part of the telescope costs.

A further interesting possibility which is emerging in Italy is the *New Hard X-ray Mission* (NHXM hereafter) designed to extend up to 80 keV the use

	NHXM		POLARIX	HXMT	XPOL
Energy range (keV)	2-10	6-35	2-10	2-10	2-10
δE at 6 keV	20%	<20%	20%	20%	20%
MDP in 100 ks (mCrab)	3% (10)	4% (10)	3.6% (10)	3% (10)	1% (1)
Ang. Res. (arcsec)	15	22	25	40	5
fov (arcmin)	12×12		15×15	25×25	2.6×2.6
Timing resolution (μs)	8		8	8	8
Telescopes	1		3	2	1
Focal length (m)	10		3.5	2.1	20
Area at 3 keV (cm^2)	520		380	610	14300

Table 1: Comparison of missions with the GPD on-board. The MDP is referred to a 100 ks observation of a source with a flux corresponding to the value reported in parentheses. In the 2-10 keV energy band, 1 mCrab corresponds to a flux $2.3 \cdot 10^{-11}$ erg/(s cm^2), while it is $2.5 \cdot 10^{-11}$ erg/(s cm^2) between 6 and 35 keV.

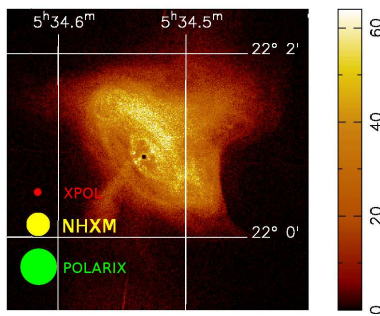


Figure 4: Angular resolution of POLARIX, NHXM and IXO compared with the Crab Nebula (background image from Weisskopf et al., 2000).

of fine angular resolution multilayer optics. The peculiarity of this mission is to perform contemporaneously imaging and spectroscopy with three identical telescopes and stacked detectors and polarimetry with a fourth optics. Two GPDs filled with mixtures of Helium/DME and Argon/DME cover the energy band 2-10 keV and 6-35 keV with a similar sensitivity, 3% and 4% for a 10 mCrab source in 100 ks respectively, and are placed alternatively in the focus of the telescope dedicated to polarimetry. The field of view is 6×6 arcmin and the angular resolution is 15 arcsec below 10 keV and 22 arcsec at 30 keV, sufficient to resolve main structures of extended sources like the Crab Nebula (see Figure 4).

5. Conclusions

X-ray polarimetry is a fundamental tool for increasing our knowledge of emission processes acting in compact sources and for investigating theories of

fundamental physics. Today gas detectors which resolve photoelectron tracks provide a valuable alternative to classical techniques of Bragg diffraction and Thomson scattering and promise to perform polarimetry of tens of galactic sources even within a small mission to be launched in a few years. The Gas Pixel Detector is in an advanced phase of development: the sensitivity expected on the basis of Monte Carlo simulations is confirmed by measurements and the detector survived irradiation, vibrations and thermo-vacuum tests. Once in-orbit with an X-ray telescope, the GPD will contemporaneously measure the polarization, the energy, the time and the direction of arrival of photons. Measurements at the level of 1% and below are within the possibility of the GPD because systematic effects are well under control thanks to the intrinsic azimuthal symmetry of the instrument. On-board of small missions, the GPD could reach between 2 and 10 keV a minimum detectable polarization of about 3% for 10 mCrab sources in 100 ks of observation and NHXM offers the possibility to extend polarimetry up to 35 keV with a similar sensitivity. The GPD will also be part of the scientific payload of the large mission IXO, whose large collecting area will allow for the measurements of polarization even of faint extragalactic sources (1% for 1 mCrab source in 100 ks) with a fine angular resolution.

Acknowledgments

The activity was supported by ASI contracts I/088/060 and I/012/08/0. The authors acknowledge the GPD team for useful discussions and suggestions.

Bellazzini, R., Spandre, G., 2010. Photoelectric polarimeters. In: X-ray Polarimetry: A New Window in Astrophysics. Cambridge University Press.

Bellazzini et al., 2003. In: Proc. of SPIE. Vol. 4843. p. 383.

Bellazzini et al., 2006. NIMA 566, 552.

Bellazzini et al., 2007. NIMA 579, 853.

Bellazzini et al., 2010 in press. A polarimeter for IXO. In: X-ray Polarimetry: A New Window in Astrophysics.

Canuto et al., 1971. Phys. Rev. D3, 2303.

Coburn, W., Boggs, S. E., 2003. Nature423, 415.

Costa et al., 2001. Nature411, 662.

Costa et al., 2006. In: Proc. of SPIE. Vol. 6266. p. 62660R.

Costa et al., 2008. In: Proc. of SPIE. Vol. 7011. pp. 70110F-1.

Costa et al., 2009. POLARIX: a pathfinder mission of X-ray polarimetry. In preparation.

Dean et al., 2008. Science 321, 1183.

- Dovčiak et al., 2008. MNRAS391, 32.
- Dyks et al., 2004. ApJ606, 1125.
- Forot et al., 2008. ApJ688, L29.
- Gambini, R., Pullin, J., 1999. Phys. Rev. D59 (12), 124021.
- Ghosh, P. K., 1983. Introduction to Photoelectron Spectroscopy. John Wiley & Sons.
- Heitler, W., 1954. Quantum theory of radiation. International Series of Monographs on Physics, Oxford: Clarendon, 1954, 3rd ed.
- Heyl et al., 2003. MNRAS342, 134.
- Hughes et al., 1984. ApJ280, 255.
- Kaaret, P., 2004. Nature427, 287.
- Lai, D., Ho, W. C. G., 2002. ApJ566, 373.
- Li et al., 2009. ApJ691, 847.
- Long et al., 1979. ApJ232, L107.
- Meszáros et al., 1988. ApJ324, 1056.
- Mitrofanov, I. G., 2003. Nature426, 139.
- Muleri et al., 2008. NIMA 584, 149.
- Muleri et al., 2009. JINST 11, 2.
- Novick et al., 1972. ApJ174, L1.
- Pavlov, G. G., Zavlin, V. E., 2000. ApJ529, 1011.
- Rees, M. J., 1975. MNRAS171, 457.
- Rutledge, R. E., Fox, D. B., 2004. MNRAS350, 1288.
- Sauli, F., 1997. NIMA 386, 531.
- Soffitta et al., 2008. In: Proc. of SPIE. Vol. 7011. pp. 701128–1.
- Stark, R. F., Connors, P. A., 1977. Nature266, 429.
- Weisskopf et al., 1978. ApJ220, L117.
- Weisskopf et al., 2000. ApJ536, L81.
- Weisskopf et al., 2009. In: Neutron Stars and Pulsars, Astrophysics and Space Science Library, Springer Berlin Heidelberg. Vol. 357. p. 589.
- Yeh, J. J., 1993. Atomic Calculation of Photoionization Cross-Sections and Asymmetry Parameters. Gordon and Breach Science Publishers, Langhorne, PE (USA).